$\Pi$ is the self-energy and has the form in this theory

$$\Pi(k^2) = i4Z_1 G^2 \int d^4q\, \Delta_{F_0}'(q^2)\Delta_{F_0}'([k-q]^2)\Gamma(k-q,q). \quad (10)$$

$\Delta_{F_0}'$ is the propagator for the $\varphi$ field, $\Gamma$ is the $\varphi^2\Phi$ vertex function. Asymptotically, $\Delta_{F_0}'(p^2) \sim 1/Z_0 p^2$ and $\Gamma \sim Z_1$, so that from (9) and (10), disregarding divergence difficulties,

$$\frac{1}{Z_c} = 4\left(\frac{Z_1 G}{Z\delta\mu^2}\right)^2 \frac{1}{Z_0} i\int d^4q\, \Delta_{F_0}'(q^2) \quad (11)$$

and in the limit as $Z \to 0$, the same result as in Ref. 1 is obtained:

$$\frac{1}{Z_c} = \frac{4\langle 0|\varphi^2(0)|0\rangle}{Z_0\lambda^2}. \quad (12)$$

I am grateful to Professor L. Castillejo and Dr. S. Zienau for informative conversations.

[1]H. M. Fried and Y. S. Jin, Phys. Rev. Letters 17, 1152 (1966).

[2]M. M. Broido and J. G. Taylor, Phys. Rev. 147, 993 (1966), and further references quoted therein.

[3]Since they correspond to different moments of the inverse propagator spectral function. $\delta\mu^2$ is shown to be nonzero in the limit $Z \to 0$ in P. Oleson, Phys. Letters 9, 277 (1964).

[4]This is the form of the propagator which appears in a general amplitude. In a composite theory, the constant term comes from an equal time commutator. This is demonstrated in the context of the Lee model by J. C. Houard, Nuovo Cimento 35, 194 (1965).

# EXPERIMENTAL TEST OF THE PION-NUCLEON FORWARD DISPERSION RELATIONS AT HIGH ENERGIES*

K. J. Foley, R. S. Jones, S. J. Lindenbaum, W. A. Love, S. Ozaki, E. D. Platner, C. A. Quarles, and E. H. Willen
Brookhaven National Laboratory, Upton, New York
(Received 26 May 1967)

We describe a critical test of the pion-nucleon forward dispersion relations up to the highest energies practical at the Brookhaven alternating-gradient synchrotron involving a precise measurement of both the real and imaginary parts of the $\pi$-$N$ scattering amplitude. We find that the predictions of the $\pi$-$N$ forward dispersion relations are in good agreement with the experiment up to at least 20 BeV/$c$.

We have measured the elastic-differential scattering of positive (8-20 BeV/$c$) and negative (8-26 BeV/$c$) pions from hydrogen at very small angles (1-25 mrad) to deduce, from the interference of the Coulomb and nuclear amplitudes, the real part of the nuclear scattering amplitude.

An earlier incomplete investigation[1] had established that there were sizable real parts of the pion-nucleon forward scattering amplitudes at high energies. However, large systematic uncertainties in the real amplitudes deduced from that experiment did not allow a definite test of the dispersion relations to be made, since such a test requires cross-section measurements with an absolute systematic accuracy better than about 1%.

The present experimental arrangement is shown in Fig. 1. The positive beam was produced at an angle of ~4° from the $F10$ target at the Brookhaven alternating-gradient synchro-

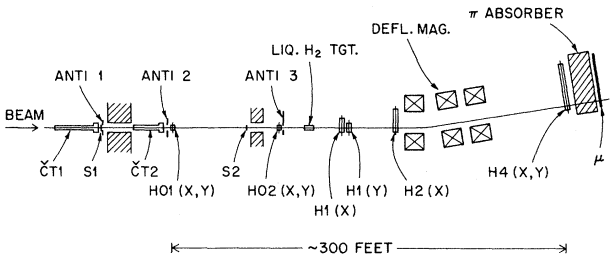


| | NUMBER OF ELEMENTS X | NUMBER OF ELEMENTS Y | DIMENSIONS (inches) WIDTH | LENGTH | THICKNESS |
|---|---|---|---|---|---|
| H01 | 12 | 12 | 0.123 | 1.5 | 0.125 |
| H02 | 10 | 10 | 0.123 | 1.25 | 0.0625 |
| H1 | 24 | 32 | 0.126 | 4.0 | 0.125 |
| | 36 | | 0.262 | 4.0 | 0.125 |
| H2 | 48 | | 0.127 | 6.0 | 0.3 |
| | 80 | | 0.266 | 6.0 | 0.3 |
| H4 | 120 | | 0.504 | 12.0 | 0.5 |
| | | 24 | 0.500 | 60.0 | 0.5 |

FIG. 1. A diagram of the experimental arrangement including a table of all hodoscope element sizes. The system had a momentum resolution of ~0.4% and an angular resolution of ~0.4 mrad.

tron (AGS), while negative particles were produced at 0° from the $F9$ target and bent on to the same path by the $F10$ AGS ring magnet. Pions were selected by the two threshold Cherenkov counters $CT1$ and $CT2$ in coincidence. Hodoscopes $H01$ and $H02$ were used to measure the location and the angle of the particle incident on the 2-ft-long hydrogen target to ±0.15 mrad. The horizontal projection of the outgoing angle after scattering in the target was measured with $H2$, while the horizontal elements of hodoscope $H4$ were used to measure the vertical projection of the outgoing angle. Hodoscope $H2$ consisted of 48 $\frac{1}{8}$-in. counters in the small-angle region and 80 $\frac{1}{4}$-in. counters covering larger angles, where the resolution was less critical. The particles passed through three $30D72$ analyzing magnets (6° bend for particles of beam momentum), and the vertical elements of $H4$ were used to measure the outgoing particle's momentum. The over-all average resolutions (rms), including beam spread, multiple scattering, counter sizes, etc., were ~0.4 mrad (angular) and ~0.4% (momentum). The hodoscopes $H1X$ and $H1Y$ were used in conjunction with $H01$, $H02$, and $H4$ to determine the location along the beam of the point of scatter in order to reject events where the interaction occurred outside the hydrogen target. The counters $\mu1$-$\mu4$, placed behind a pion absorber consisting of 6 ft of steel and 2 ft of lead followed by 2 ft of paraffin, were used to reject muons from decays along the beam. By raising 8 ft of iron into the beam at the hydrogen target, a broad-muon beam was produced and used to measure the efficiency of muon rejection as a function of position in $H4$. For all regions used, it was greater than 95% efficient, resulting in a muon contamination of less than 0.25%. The over-all particle detection efficiency of the spectrometer system was measured at each momentum by bending the beam onto $H4$. By triggering on the incident beam, we were then able to measure the probability that a well-defined particle would traverse the spectrometer and be recorded as a single particle in each screen. From the observed variation of this efficiency, after correction for the energy-dependent muon contamination and pion decay, we concluded that the over-all absolute normalization is correct to within 1%. In order to reduce accidentals, events in which more than one incident hodoscope counter per screen was struck were vetoed electronically. The net accidental corrections were always less than 1%. The method of data handling is very similar to that described in earlier papers.[2] A fast (5-nsec) coincidence between $S1$, $S2$, $\bar{A}1$, $\bar{A}2$, $\bar{A}3$, $H01$, $H02$, $CT1$, and $CT2$ was used to identify the incident particles. A further 20-nsec coincidence with $H2$ and $H4$ determined that the particle had scattered into a selected fiducial region. When such a coincidence signal was received, 144 fast gates were opened for 20 nsec to identify which of the counters had been struck.[3] This information was then transferred to a buffer memory, and 15 μsec later the system was ready to receive another event. Up to 2000 such events were recorded each pulse (~3 million/h). At the end of the AGS pulse, the data in the buffer memory was transferred to a PDP 6 computer for on-line analysis and in parallel onto magnetic tape for a permanent record. The computer program calculated the scattering angle and momentum of each particle and constructed momentum spectra for each of 30 scattering angle bins of width 0.4 to 1 mrad. Counter performances were monitored during the data taking by constructing histograms of count rate versus counter number for each screen. The magnetic fields of the beam transport were monitored by the computer on a pulse by pulse basis.

At larger angles the empty target background was ~10%, but at the smallest angles, where the position of the interaction along the beam was not well determined, it became as large as 50%. Frequent empty target measurements were made at each momentum, so that the empty-target background could be subtracted accurately.

Differential cross sections were obtained by integrating the momentum spectra from hydrogen over the elastic peak and subtracting the small (≲1%) nonelastic background. The effective values of $t$ (the negative square of the four-momentum transfer) for the various bins were determined by means of a Monte Carlo program which constructed events using the known geometry, incident-particle distribution, and momentum spread. Typical cross sections are shown in Fig. 2. The errors shown are largely statistical, but point-to-point systematic errors due to uncertainty in the determination of $t$ and the measured nonuniformity of $H2$ and $H4$ are included. An uncertainty in the over-all absolute normalization of 1% is not

shown.

Invariance principles limit the $\pi$-$p$ scattering amplitude to a form involving two complex functions:

$$A_N(s,t)=f(s,t)+g(s,t)\vec{\sigma}\cdot\vec{n}\sin\theta. \quad (1)$$

For the small angle range where interference takes place, $\sin\theta \ll 1$. Considering the limits on the spin-flip amplitude as determined by the characteristics of the $\pi$-$p$ polarization and differential cross-section data, neglecting the spin-flip amplitude causes a negligible error in the small-angle region we are concerned with and hence $A(s,t)=f(s,t)$.

We express the differential cross section as

$$\frac{d}{dt}\sigma(\pi^{\pm}\text{-}p)=\frac{F_c^2}{t^2}\mp\frac{2F_c}{|t|}\mathrm{Im}(A_{N\pm})[\alpha_{\pm}\cos2\delta\pm\sin\delta]+[1+\alpha_{\pm}^2][\mathrm{Im}(A_{N\pm})]^2+\text{mult. scatt. corr.}, \quad (2)$$

where $\alpha=\mathrm{Re}(A_N)/\mathrm{Im}(A_N)$ and $F_C=(2\pi^{1/2}e^2/\beta c)$ $\times$ (form factor).

Bethe[4] has calculated $\delta=(e^2/\hbar c\beta)\ln(1.06/pa\theta)$. In a number of recent works,[5,6] the calculation of $\delta$ has been investigated in detail. Three of the calculations[5] agree within 15% with the above result. The major difference in the fourth calculation[6] is due to the neglect of a form factor effect in making the infrared approximation.[7] Since the exponential slope or equivalent radius of the $\pi$-$p$ interaction is about the same as for $p$-$p$, we have used the proton form factor[8] for the pion. The effect of the form factor is very small in the region of interest, and the uncertainty in it introduces a negligible error.

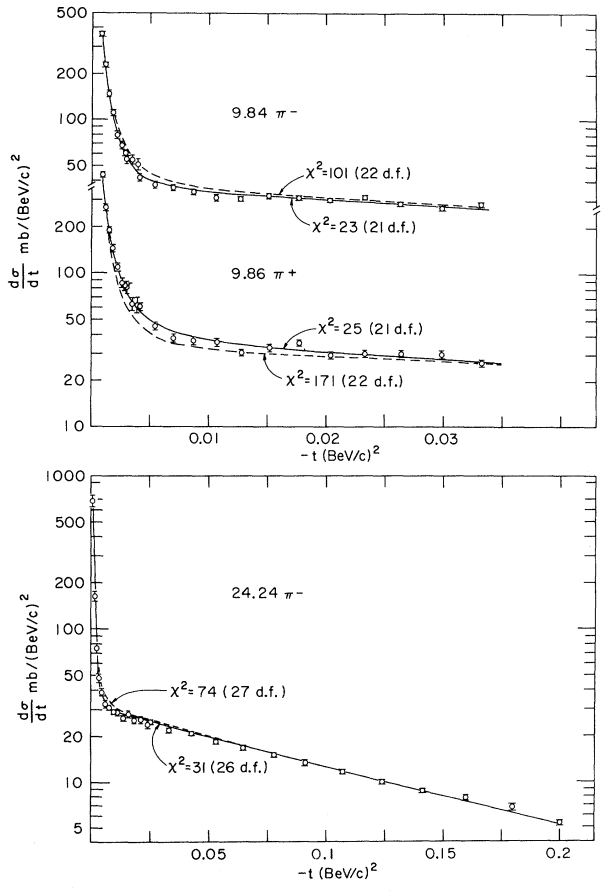


FIG. 2. Typical differential cross sections. The 9.86 $\pi^+$ data are displaced down one decade. The solid curves are best fits varying $\alpha$ and $b$. The dashed curves are best fits constraining $\alpha$ to be 0. The number of degrees of freedom (d.f.) of each fit is shown.

Multiple and plural scattering corrections were calculated by using a modified Molière distribution.[9] We express

$$|A_N|^2=(1+\alpha^2)\frac{(\sigma_{\mathrm{tot}})^2}{16\pi\hbar^2}e^{bt+ct^2},$$

where $ct^2$ is a small correction to the nearly exponential behavior of the differential scattering cross section. We used $c=2.4$ (BeV/$c$)$^{-4}$ as an average value from larger $|t|$ measurements.[10] Total cross-section measurements were made as a separate part of this experiment[11] from 8 to 22 BeV/$c$ for $\pi^+$-$p$ and from 8 to 29 BeV/c for $\pi^-$-$p$ at about 2 BeV/$c$ intervals.

The measured differential cross sections have been fitted at each momentum, using $\alpha$ and $b$ as free parameters. The solid curves in Fig. 2 show the best fit to the data obtained; the dotted curve is the best fit with $\alpha=0$, which is ruled out by $\chi^2$. The interference is destructive for $\pi^-$-$p$ and constructive for $\pi^+$-$p$. The value of $\alpha$ is very insensitive to the minimum value of $|t|$ used in the fit. This shows that the parametrization used, including the assumption of no $t$ dependence of $\alpha$, was reasonable. A minimum cutoff at $|t|\approx 0.001$ (BeV/$c$)$^2$ was selected for the final determinations. That the value of $\alpha$ determined then corresponds to the

Table I. $\alpha = \mathrm{Re}(A_N)/\mathrm{Im}(A_N)$ for $\pi^{\pm}$-$p$ scattering. The errors do not include a scale error of ±0.02 as described in the text. The starred momenta were measured with a set-up covering a larger angular region.

| $\pi^-$-$p$ Momenta (BeV/$c$) | $\alpha_-$ | $\pi^+$-$p$ Momenta (BeV/$c$) | $\alpha_+$ |
|---|---|---|---|
| 7.89* | −0.149 ± 0.021 | 7.76* | −0.225 ± 0.019 |
| 9.84 | −0.124 ± 0.017 | 9.86 | −0.223 ± 0.019 |
| 9.89* | −0.167 ± 0.020 | 10.02* | −0.215 ± 0.010 |
| 11.89 | −0.137 ± 0.017 | 11.95* | −0.185 ± 0.018 |
| 14.16 | −0.131 ± 0.025 | 14.00 | −0.187 ± 0.021 |
| 15.99 | −0.143 ± 0.018 | 16.02* | −0.169 ± 0.017 |
| 16.00* | −0.144 ± 0.022 | | |
| 18.19* | −0.112 ± 0.024 | 17.96 | −0.139 ± 0.022 |
| 20.15 | −0.117 ± 0.025 | 20.19 | −0.144 ± 0.031 |
| 20.38 | −0.132 ± 0.017 | | |
| 22.13 | −0.123 ± 0.026 | | |
| 24.24 | −0.125 ± 0.027 | | |
| 26.23 | −0.128 ± 0.026 | | |

value at $t = 0$ is well justified.[12] Measurements at $|t| > 0.04$ (BeV/$c$)$^2$ have little weight in the determination of $\alpha$. The values of $b$ obtained were consistent with previous measurements.[10] The values of $\alpha$ obtained are given in Table I and are shown in Fig. 3. The solid points represent measurements with the apparatus rearranged to cover a larger angular range with consequent worse resolution. The data were grouped in angular bins about 50% wider. As can be seen, the agreement between the two setups is good. The errors shown are those

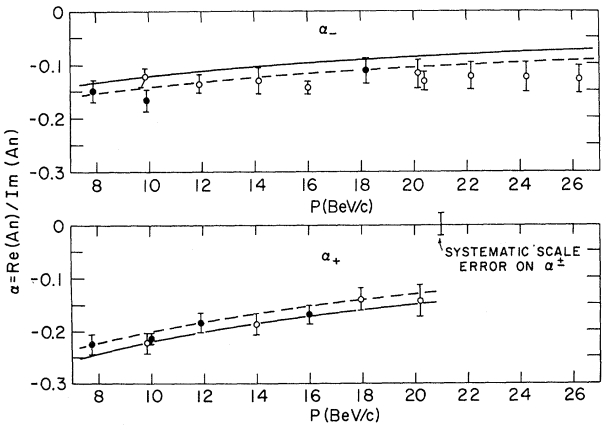


FIG. 3. $\alpha_{\pm}$ versus momentum. The solid curves are predictions of dispersion relations discussed in the text. The dashed curve is the result of displacing the solid curve by 0.02, the systematic scale error. The solid points represent measurements with a rearrangement of the apparatus to cover a larger angular range.

obtained from the lease-squares fit. In addition, there is an over-all systematic error in $\alpha$ of ±0.02 due to the following: (1) uncertainty in total cross-section measurements, (2) inelastic background subtraction, (3) uncertainty in overall efficiency, and (4) uncertainty in the multiple scattering corrections.

This error is mostly of a scale nature, and since the sign of the interference is opposite for $\pi^+$ and $\pi^-$, the sum of the values of $\alpha$ for $\pi^+$ and $\pi^-$ at any momentum is nearly free of this error.

Although these new results for $\alpha$ differ considerably from our earlier incomplete determination,[1] considering the large systematic errors assigned to the earlier measurements, there is no significant disagreement. Because of the greatly imporved absolute accuracy and resolution of these measurements, resulting in lower backgrounds and better $t$-cutoff dependence, these data should supersede the earlier measurements.

The predictions of the $\pi$-$p$ forward dispersion relations[13] were evaluated from the following well-known forms:

$$D^+(\omega) = D^+(\mu) + \frac{f^2 k^2}{M[1-(\mu/2M)^2]} \frac{1}{\omega^2 - (\mu^2/2M)^2} + \frac{k^2}{4\pi^2} P\int_\mu^\infty \frac{d\omega'}{k'} \frac{\omega'}{\omega'^2 - \omega^2}(\sigma_- + \sigma_+), \quad (3)$$

$$D^-(\omega) = \frac{2f^2\omega}{\omega^2 - (\mu^2/2M)^2} + \frac{\omega}{4\pi^2} P\int_\mu^\infty d\omega' \frac{k'}{\omega'^2 - \omega^2}(\sigma_- - \sigma_+), \quad (4)$$

where $D^{\pm} = \frac{1}{2}[\mathrm{Re}(A_N-) \pm \mathrm{Re}(A_N+)]$, $\sigma_{\pm}$ are the $\pi^{\pm}p$ total cross sections, and natural units $\hbar = c = 1$ have been employed. The values $f^2 = 0.081$ and $D^+(\mu) = -0.002$ were used, the results being insensitive to reasonable variations in these parameters and the lower-energy total cross-section measurements.

A least-squares fit to the new high precision (~0.3% absolute accuracy) total cross-section measurements[11] of the form $\sigma_{\pm} = a + b_{\pm}/p^{n}{}_{\pm}$ was used to evaluate the dispersion integrals above 8 BeV. The parameters used were $a = 22.72$, $b_+ = 28.99$, $b_- = 20.33$, $n_+ = 1.128$, and $n_- = 0.697$.

The predictions for $\alpha_{\pm}$ from this fit are shown as solid lines on Fig. 3. The dashed lines reflect the estimated systematic errors of the $\alpha$ measurements.

As can be seen in Fig. 3, the agreement with

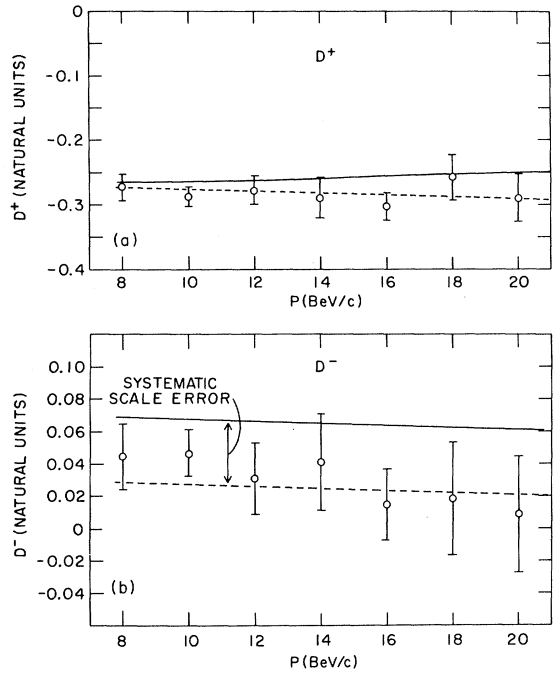


FIG. 4. (a) $D^+$ versus momentum. The solid curve is the prediction of the dispersion relations using the best fit to the total cross section for extrapolation. The dotted curve is the result of a subtraction at 20 BeV/$c$. (b) $D^-$ versus momentum. The solid curve is the prediction of the dispersion relations as in Fig. 4(a). The dashed curve is the result of displacing the solid curve by 0.04, the systematic scale error.

the predicted shapes of $\alpha_-$ and $\alpha_+$ is good, and considering the systematic errors, the agreement of the absolute magnitude is satisfactory. The curve is the result of an extrapolation of the best fit to the total cross-section measurements. Within the total cross-section errors, this extrapolation can be adjusted to give an even better agreement between the predictions and the data.

All important systematic errors, including the uncertainty in $\delta$, tend to make about equal and opposite contributions to $\alpha_-$ and $\alpha_+$, and hence they must, to a large extent, cancel in the quantity $D^+$, providing a more precise test of the forward dispersion relations.

Figure 4(a) shows this comparison and we see that the agreement is good. If the total cross section obeys the Froissart bound, the dispersion integral is convergent without an additional subtraction. However, in order to reduce greatly the sensitivity of the integral to the high energy cross section beyond the measured momentum range, an additional subtraction in $D^+$ was made at 20 BeV/$c$ and the result is shown as a dotted line in Fig. 4(a). The agreement is improved. Since in this form the dispersion-relation prediction is virtually independent of the high-energy behavior of the total cross sections,[14] we conclude that the $D^+$ forward dispersion relation is valid up to 20 BeV/$c$.

Figure 4(b) shows a comparison between the prediction for $D^-$ and the experimentally determined values. Here the systematic errors add; so we do not have as good a determination. Furthermore, $D^-$ is very sensitive to the asymptotic behavior of the difference of the total cross sections which, of course, is not measured as well as the sum.[15] Within the errors, the agreement is satisfactory.

The charge exchange data[16] are also in agreement with predictions from our data, within the systematic error limits, assuming the hypothesis of charge independence. Therefore, the experimental data up to BeV/$c$ are consistent with the assumption of charge independence.

In conclusion, the excellent agreement obtained between the $\pi$-$p$ forward dispersion-relation predictions and these experimental results provides a critical verification of the validity of the dispersion relations up to the highest energies measured. If a small acausal region or "fundamental length" $l_0$ existed, the forward dispersion relations would break down completely at an energy $\sim 1/l_0$.[17] Applying this to our present results, we obtain $l_0 < 10^{-15}$ cm.

The authors wish to thank the AGS staff and the operators and experimental support groups for their generous cooperation and valuable assistance during the performance of this experiment. We also wish to acknowledge the assistance of the Brookhaven National Laboratory On-Line Data Facility staff and our group technicians.

---

*Work performed under the auspices of the U. S. Atomic Energy Commission.

[1]K. J. Foley, R. S. Gilmore, R. S. Jones, S. J. Lindenbaum, W. A. Love, S. Ozaki, E. H. Willen, R. Yamada, and L. C. L. Yuan, Phys. Rev. Letters 14, 862 (1965).

[2]K. J. Foley, W. Higinbotham, S. J. Lindenbaum, W. A. Love, S. Ozaki, D. Potter, and L. C. L. Yuan, in "Proceedings of the CERN International Meeting on Film-less Spark Chamber Techniques and Associated Computer Use," CERN Report No. CERN 64-30, 1964 (unpublished), p. 21; K. J. Foley, R. S. Gilmore, R. S. Jones, S. J. Lindenbaum, W. A. Love, S. Ozaki, E. H. Willen, R. Yamada, and L. C. L. Yuan, in Proceed-

ings of the Twelfth International Conference on High Energy Physics, Dubna, 1964 (Atomizdat., Moscow, 1966), p. 418.

[3]A system for multiplexing the photomultiplier signals were used such that the outputs of ~400 phototubes were reduced to 144 bits of information. For instance, the 120 counters of *H4X* were encoded as 10 groups of 12 counters, thus requiring a total of 22 bits.

[4]H. A. Bethe, Ann. Phys. (N.Y.) 3, 190 (1958).

[5]J. Rix and R. M. Thaler, Phys. Rev. 152, 1357 (1966); M. M. Islam, Report No. NYO-2262TA-149, and private communications; R. Serber, private communication.

[6]L. D. Solov'ev, Zh. Eksperim. i Teor. Fiz. 49, 292 (1965) [translation: Soviet Phys.—JETP 22, 205 (1966)].

[7]D. R. Yennie, private communication.

[8]L. N. Hand, D. G. Miller, and R. Wilson, Rev. Mod. Phys. 35, 335 (1963).

[9]G. Molière, Z. Naturforsch. 3A, 78 (1948); H. A. Bethe, Phys. Rev. 89, 1256 (1953); U. Fano [Phys. Rev. 93, 117 (1954)] has calculated the correction for the fact that the atomic electrons cannot scatter pions through an angle greater than 3.7 mrad.

[10]K. J. Foley, S. J. Lindenbaum, W. A. Love, S. Ozaki, J. J. Russell, and L. C. L. Yuan, Phys. Rev. Letters 10, 543 (1963); K. J. Foley, R. S. Gilmore, S. J. Lindenbaum, W. A. Love, S. Ozaki, E. H. Willen, R. Yamada, and L. C. L. Yuan, Phys. Rev. Letters 15, 45 (1965).

[11]To be published.

[12]To produce even a 5% change in $\alpha$ on extrapolating from $|t| = 0.001$ (BeV/$c$)$^2$ to $t = 0$ would require an exponential slope of the real amplitude greater than 100 (BeV/$c$)$^{-2}$, corresponding to diffraction from an object of radius 3 F. Such a range of interaction would be in disagreement with many experimental measurements. At the lower energies where cross sections at smaller $t$'s could be measured, even including the measurements to $|t| = 0.0001$ (BeV/$c$)$^2$ made no observable difference in the value of $\alpha$, confirming the validity of this argument.

[13]M. L. Goldberger, Phys. Rev. 99, 979 (1959); M. L. Goldberger, H. Miyazawa, and R. Oehme, Phys. Rev. 99, 986 (1955).

[14]Even assumptions of drastic behavior, such as a sum of the cross sections which suddenly vanishes and remains 0 above 35 BeV/$c$ or alternately a sum that increases linearly with energy beyond 35 BeV/$c$, make only small differences in the predictions for the experimentally measured energy range.

[15]An equally good fit to the total cross sections using the same number of parameters is $\sigma_+ + \sigma_- = 44.20 + 18.4/p^{0.69}$ and $\sigma_- - \sigma_+ = 3.85/p^{0.306}$. This fit gave similar predictions for $D^+$ but gave results for $D^-$ which disagreed with the data because of the slower convergence of the total cross section difference at high energies. However, a two-standard-deviation change in the exponent of the momentum dependence of this fit would give a reasonable agreement with $D^-$.

[16]I. Menelli, A. Bigi, R. Carrara, M. Wahlig, and L. Sodickson, Phys. Rev. Letters 14, 408 (1965); A. V. Stirling, P. Sonderegger, J. Kirz, P. Falk-Vairant, O. Guisan, C. Bruneton, P. Borgeaud, M. Yvert, J. P. Guillaud, C. Caverzasio, and B. Amblard, Phys. Rev. Letters 14, 763 (1965).

[17]R. Oehme, Phys. Rev. 100, 1503 (1955); D. I. Blokhintsev, Usp. Fix. Nauk 89, 185 (1966) [translation: Soviet Phys.—Usp. 9, 405 (1966).

## PROTON AND PION SPECTRA FROM PROTON-PROTON INTERACTIONS AT 10, 20, AND 30 BeV/$c$*

E. W. Anderson, E. J. Bleser, G. B. Collins, T. Fujii,† J. Menes, and F. Turkot
Brookhaven National Laboratory, Upton, New York

and

R. A. Carrigan, Jr., R. M. Edelstein, N. C. Hien, T. J. McMahon, and I. Nadelhaft
Carnegie Institute of Technology, Pittsburgh, Pennsylvania

(Received 21 March 1967)

The secondary proton and pion spectra from proton-proton interactions have been measured over nearly the entire momentum range and over a wide range of laboratory angles. Most of the data are at an incident-proton momentum of 30 BeV/$c$.

The proton spectra were transformed into cross sections in terms of $p_\perp$* and $p_\parallel$* all in the c.m. system. These cross sections were found to be largely independent of $p_\parallel$* and an empirical fit was obtained quite similar to one derived by Hagedorn using a statistical model. The pion spectra were also expressed in terms of $p_\perp$* and $p_\parallel$* and found to be different from the proton spectra by showing a marked dependence on $p_\parallel$*.

As part of a proton-proton scattering experiment reported earlier,[1,2] we obtained spectra of secondary protons and pions covering a wide range of angles and momenta. A description of the wire-plane spectrometer system and analysis procedure is found elsewhere.[3] Separation of protons and $\pi^+$ mesons was accomplished with a 7-ft-long, freon-filled, threshold Cherenkov counter operating at pressures between 15 and 35 psi. The efficiency of this